

# Manipulation of individual water molecules on CeO<sub>2</sub>(111)

S Torbrügge<sup>1</sup>, O Custance<sup>2</sup>, S Morita<sup>3</sup> and M Reichling<sup>1</sup>

<sup>1</sup> Fachbereich Physik, Universität Osnabrück, Barbarastr. 7, 49076 Osnabrück, Germany

<sup>2</sup> National Institute for Materials Science, 1-2-1 Sengen, 305-0047 Tsukuba, Ibaraki, Japan

<sup>3</sup> Graduate School of Engineering, Osaka University, 2-1 Yamada-Oka, 565-0871 Suita, Osaka, Japan

E-mail: [reichling@uos.de](mailto:reichling@uos.de)

Received 30 August 2011, in final form 11 October 2011

Published 7 February 2012

Online at [stacks.iop.org/JPhysCM/24/084010](http://stacks.iop.org/JPhysCM/24/084010)

## Abstract

Water molecules adsorbed on the CeO<sub>2</sub>(111) surface are investigated by non-contact atomic force microscopy (NC-AFM) at several tip-sample temperatures ranging between 10 and 300 K. Depending on the strength of the tip-surface interaction, they appear as triangular protrusions extended over three surface oxygen atoms or as small pits at hollow sites. During NC-AFM imaging with the tip being close to the surface, occasionally the transfer of molecules between tip and surface or the tip-induced lateral displacement of water molecules to equivalent surface lattice sites is observed. We report how this situation can be exploited to produce controlled lateral manipulations. A protocol to manipulate the water molecules between pre-defined neighbouring equivalent adsorption sites of the regular lattice as well as across a surface oxygen vacancy is demonstrated.

(Some figures may appear in colour only in the online journal)

## 1. Introduction

The controlled positioning of individual atoms and molecules on a surface is one of the grand endeavours in nanoscience [1], that has been turned into reality with the advent of scanning tunnelling microscopy (STM) [2]. The technique has been developed to perfection, and precise atomic and molecular manipulation on metallic substrates at cryogenic temperatures has been demonstrated for a large number of species [3–5]. Extending such studies to semiconducting surfaces lifted the restriction of low temperatures and established room temperature molecular manipulation [6–8]. Any of such manipulation processes is the result of a force exerted by the probe forefront apex over the manipulated species [2]. The tunnelling conductance measured in a STM experiment has been predicted to be proportional to the square of the tip-surface interaction energy [9]; however, this relation is still under strong debate [10–12] and, so far, the STM can only provide indirect evidence of the forces involved in atomic manipulation processes [13]. On the other hand, the atomic force microscope (AFM) operated in non-contact mode (NC-AFM) allows a direct quantification

of the forces involved in atomic manipulation [14]. In addition, the AFM allows the investigation of atomic and molecular processes on electrically insulating substrates that are not accessible to the STM. Techniques for the precise manipulation of atoms and adsorbates at surfaces have also been developed for the AFM [15], and several sophisticated and well documented protocols for precise vertical [16–18] and lateral [19–21] manipulation of atoms at semiconductor surfaces have been demonstrated. The final objective in this field, however, is controlled manipulation on electrically insulating substrates. In the very few examples investigated so far, the relation between the binding energy of the manipulated species and the characteristic diffusion barriers has been found to facilitate lateral manipulations at room temperature on insulating surfaces. In preliminary experiments, this has been demonstrated for defects on the KCl(100) surface [22] and water molecules on the CaF<sub>2</sub>(111) surface [23], where very characteristic manipulation patterns have been observed. However, the precision and degree of control in these manipulation experiments on insulating substrates is not nearly as well developed as for AFM manipulations at semiconductor surfaces [15], and the manipulation mechanisms are still not well understood.

Here we introduce the controlled manipulation of individual water molecules on  $\text{CeO}_2(111)$ , the most stable surface of a material that is of great interest for many applications in heterogeneous oxidation catalysis [24–27], especially in the form of nanoparticles. Ceria ( $\text{CeO}_2$ ), among other members of the family of reducible oxides, has already been quite well characterized by NC-AFM [28], having revealed details of the surface morphology [29, 30], atomic contrast formation [31], and the structure of surface and sub-surface oxygen vacancy defects [32] on the (111) face. However, a striking observation has been the room temperature adsorption of water molecules on flat terraces of the stoichiometric surface. The respective experimental demonstration [33] has basically been confirmed by theoretical simulations [34, 35]. This is in contrast to the more complicated case of the  $\text{H}_2\text{O}/\text{CaF}_2(111)$  system ( $\text{CeO}_2(111)$  and  $\text{CaF}_2(111)$  are structurally very similar), where molecular water can be stabilized only by surface defects, being extremely mobile on the stoichiometric surface and, therefore, not accessible to room temperature NC-AFM imaging [36].

In the present study of water on  $\text{CeO}_2(111)$ , we first focus on details of NC-AFM contrast appearance when imaging water molecules at different tip–surface distances. Depending on the interaction strength, we observe a characteristic imaging contrast that is a key to the understanding of the features observed during the manipulation of individual water molecules. We then explore how water molecules can be moved across the surface by scanning at reduced tip–surface distances from standard NC-AFM imaging, and apply a manipulation protocol allowing for the precise positioning of individual water molecules on pre-defined accessible positions on the surface. Finally, we demonstrate that controlled manipulation of individual water molecules is not only possible on stoichiometric terraces but also across a surface vacancy on a slightly reduced crystal.

## 2. Experimental procedures

Experiments are carried out in two different ultra-high vacuum (UHV) AFM systems depending on the desired range of sample temperature. For room temperature experiments we used a modified commercial AFM that has been described in detail elsewhere [37]. Experiments at low temperatures were carried out with a home-built UHV AFM, using liquid nitrogen and liquid helium as coolants for reaching temperatures of 80 K and 10 K, respectively. In this instrument, the entire scan head and the sample are kept at precisely the same temperature as they are enclosed in a bath cryostat. In both systems, the residual gas pressure is below  $1.3 \times 10^{-8}$  Pa. Water exposure was accomplished by backfilling the UHV chamber with water vapour: ultra-clean Milli-Q water, further purified by several freeze–pump–thaw cycles, was introduced into the UHV chamber via a leak valve. The composition of the residual gas in the UHV system and the partial pressure of water during dosage were monitored with a quadrupole mass analyser. To obtain a stoichiometric or slightly defective  $\text{CeO}_2(111)$  surface, sputter cleaning

and annealing cycles were applied as has been described previously [29]. As force sensors, we used commercial silicon cantilevers (Nanoworld AG, Neuchâtel, Switzerland) with highly effective  $Q$ -factors [38] and force constants  $k$  specified in the figure captions. Tips were prepared *in situ* by  $\text{Ar}^+$  ion sputtering prior to the experiments, to remove the native oxide layer. However, in some occasions, tip apexes providing atomic contrast in NC-AFM imaging were also formed by scanning over step-edges or by gently contacting the tip with the surface, resulting in the deposition of material from the tip.

Imaging was performed in the constant frequency shift mode, where the shift from the fundamental resonance frequency  $f_0$  of the cantilever due to the tip–surface interaction is kept constant at a certain imaging set point  $\Delta f$  [29], and the oscillation amplitude  $A$  of the cantilever was kept constant at any time. The tip–surface electrostatic interaction was minimized by compensating the tip–surface contact potential difference measured  $\sim 2$  nm above the explored surface area [39, 40]. It is believed that the hexagonal arrangement of bright spots seen in our NC-AFM images of the bare  $\text{CeO}_2(111)$  surface represents the atomic structure of the top-most oxygen lattice terminating the surface [31]. The data presented here were obtained over several measurement sessions using different cantilevers, and therefore different tip terminations. Consequently, set points for imaging and manipulation experiments performed with different cantilevers—characterized by a distinct fundamental resonance frequency—are not directly comparable.

## 3. Water adsorption and NC-AFM contrast of individual water molecules

In previous works, we have reported the general morphology of the  $\text{CeO}_2(111)$  surface upon water exposure at room temperature [33], and interpreted triangular protrusions extending over three oxygen atoms of the  $\text{CeO}_2(111)$  surface (figure 1) as individual water molecules. This characteristic appearance contrasts with the elusive tiny features observed upon water adsorption on  $\text{CaF}_2(111)$  [23] or with the structure resolved by STM measurements on metals like  $\text{Pd}(111)$  [41], for instance. To elucidate NC-AFM contrast formation of water on  $\text{CeO}_2(111)$  in more detail, we have performed an extended study on water molecules imaged under varied experimental conditions. Figures 1(a)–(c) display NC-AFM images of individual water molecules taken at temperatures of 10, 80 and 300 K, respectively. These images qualitatively show the same result: under regular imaging conditions, surface oxygen atoms appear as circular protrusions [31] while individual water molecules are visualized as triangular features extending over three nearest neighbour oxygen atoms and presenting an orientation that is always the same [33]. As shown in figure 1(d), water molecules can also be seen adsorbed in a position adjacent to a surface oxygen vacancy [32]; however, we have never observed a water molecule directly occupying a vacancy site.

Theoretical modelling of the adsorption of water on  $\text{CeO}_2(111)$  yields that the molecule dissociates and the

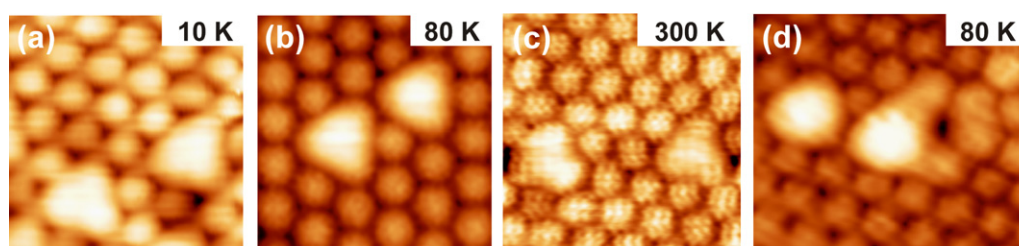


**Figure 1.** Water molecules adsorbed on stoichiometric CeO<sub>2</sub>(111) imaged at (a) 10 K, (b) 80 K and (c) 300 K. (d) Water molecules adsorbed at positions close to a surface oxygen vacancy measured at 80 K. Image sizes (a)–(c) (2.5 × 2.5) nm<sup>2</sup>, (d) (2.5 × 2.0) nm<sup>2</sup>. Acquisition parameters (a)  $f_0 = 170\,707.2$  Hz,  $A = 11.5$  nm,  $k = 34.8$  N m<sup>-1</sup>,  $\Delta f = -69$  Hz; (b)  $f_0 = 150\,940$  Hz,  $A = 7.1$  nm,  $k = 24.6$  N m<sup>-1</sup>,  $\Delta f = -32.9$  Hz; (c)  $f_0 = 83\,898$  Hz,  $A = 36.4$  nm,  $k = 2.8$  N m<sup>-1</sup>,  $\Delta f = -19.4$  Hz; (d)  $f_0 = 162\,896$  Hz,  $A = 8.7$  nm,  $k = 30.9$  N m<sup>-1</sup>,  $\Delta f = -74.7$  Hz.

resulting proton may attain three equivalent neighbouring positions around the binding site occupied by the hydroxyl left over from the water molecule. A small energetic barrier between the three equivalent configurations has been predicted [34]. A plausible hypothesis for the triangular features observed in figure 1 would be that the contrast originates from a superposition of contributions to the tip–surface interaction during the time that the molecule visits each of the three equivalent configurations available around a hollow site between three surface oxygen atoms, resulting in a quasi-rotational movement of the molecule. Similar behaviour has been detected, for instance, for the adsorption of individual Pb atoms on the Si(111)-(7×7) surface [42]. The fact that the contrast does not change even when imaging at temperatures as low as 10 K (figure 1(a)) points towards either a very small activation barrier for the movement of the molecule that can be overcome by thermal excitations at 10 K or to a rotation enhanced by the interaction with the tip during the imaging process. Extended theoretical modelling of the tip–surface interaction during scanning, including possible tip and surface relaxations, molecular deformations and the influence of the tip on the water adsorption, is needed to yield a further understanding of the observed contrast.

The NC-AFM image contrast reversibly changes when the tip–surface interaction is increased, as demonstrated in figure 2, where a series of 14 images recorded at a temperature of 80 K over the same water molecule is shown. In frame (1), the water molecule is imaged at a typical set point for atomic resolution imaging of the CeO<sub>2</sub>(111) surface. The shape of the water molecule is similar to the features displayed in figure 1. It appears as a triangular protrusion about 75 pm higher than the oxygen layer, and extends over three nearest neighbouring surface oxygen atoms. This image and the corresponding set point were used as a reference, so that after recording each of the images composing the series, we carefully checked that we obtained the same contrast when imaging at the reference set point. This ensures reproducible imaging conditions, evidences the stability of the molecule, and specifically excludes that the results are compromised by tip changes that would result in a significant change in contrast. The series of images shown in figure 2 reveals that upon increasing the tip–surface interaction, the triangular protrusion ascribed to the water molecule gradually vanishes, and a pit progressively appears at the hollow site between

the three oxygen atoms over which the feature of the water molecule extends. In frame (14), recorded at the highest tip–surface interaction within the series, the water molecule is merely imaged as a small black triangle about 100 pm deep with respect to the unperturbed oxygen layer and, in contrast to the reference image, the three surface oxygen atoms over which the molecule extends are clearly visible.

The central pit evolves from a stripe in the fast scanning direction as highlighted in frame (4'), which is frame (4) displayed with a different colour scale. Similar phenomena detected on molecular adsorbates have been described as a contrast inversion due to a difference in the distance dependence of the tip–surface interaction on and beside the molecule [43]. However, in this case, the successive development of the central pit upon increasing the tip–surface interaction is likely to be due to a significant local reduction of tip–surface short-range interaction at the position in which the water molecule is strongly bound to the surface. The visualization of the three oxygen atoms over which the triangular feature of the water molecule extends can be understood as an avoidance of the water molecule under the force field induced by tip. The presence of the tip at reduced tip–surface separations over the site associated with one of the three equivalent neighbouring configurations available for the water molecule [34] during the tip scan may prevent the water molecule from visiting that particular surface location. The tip–surface short-range interaction would then be dominated by the interaction between the tip forefront atom and the surface oxygen atoms underneath the triangular feature ascribed to the water molecule. In this way, the three oxygen atoms otherwise blurred by the water feature can clearly be imaged by the AFM (see frames (1) and (14) and their comparison (1) & (14) in figure 2). Under the imaging conditions for the series depicted in figure 2, the molecular feature is stably adsorbed at the hollow site between three surface oxygen atoms, and only upon increasing the tip–surface interaction even further it is possible to induce the displacement of the molecule to a neighbouring binding site.

#### 4. Tip-induced movement of water molecules during NC-AFM imaging

When imaging above a particular tip–surface interaction threshold, it is frequently observed that the water molecules

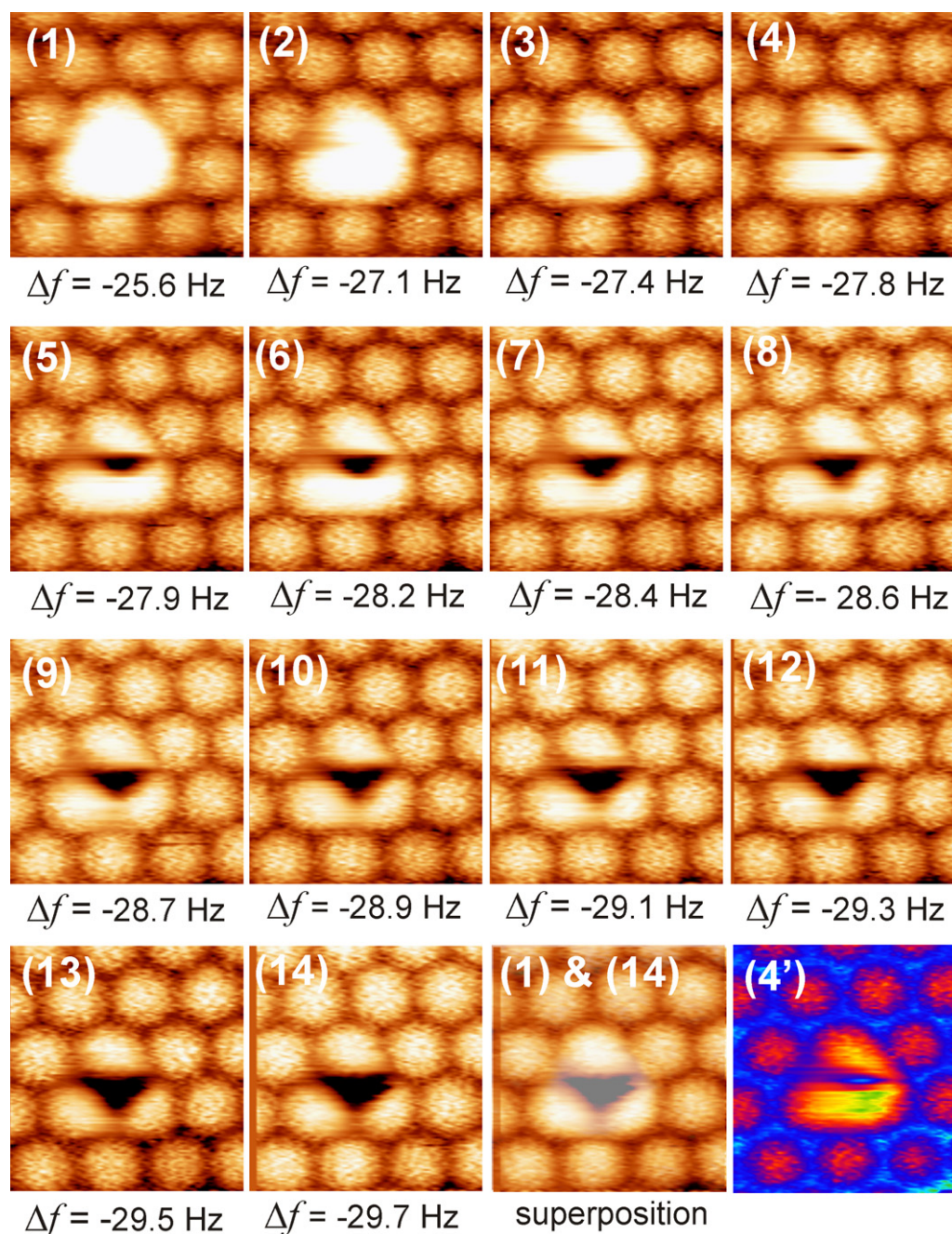


**Figure 2.** Series of topographic images acquired over the same water molecule at 80 K upon increasing the tip–surface interaction. Images were acquired from top to bottom with the fast scan direction from left to right, lifting the tip up by several angstroms on the way back. The numbers within the frame correspond to the successive imaging sequence. The imaging set point is given below each image. Figure (1) & (14) is a superposition of figure (1) and (4), each of them contributing 50% of the total contrast. Figure (4') is figure (4) displayed with a different colour scale. Image size  $(1.5 \times 1.5)$  nm<sup>2</sup>. Acquisition parameters  $f_0 = 150\,940$  Hz,  $A = 7.1$  nm,  $k = 24.6$  N m<sup>-1</sup>.

diffuse on the surface following the tip. This is illustrated by the series of images shown in figure 3, where a water molecule is dragged by the tip during regular scanning of the surface. All images displayed in figure 3 are scanned from top to bottom (slow scan direction) while individual lines (fast scan direction) are performed under equal conditions in forward and backward direction.

In figure 3(a), a water molecule and the surrounding surface atoms are imaged at a standard set point for imaging

with the tip used in this series of experiments; this results in imaging the water molecule as an unperturbed bright triangular protrusion. A displacement of the molecule is induced when the tip is brought closer to the surface. In the image of figure 3(b), the water molecule appears as a truncated dark pit at its original adsorption position, and a second time at an equivalent binding site shifted by one lattice constant; which is testament to the displacement of the molecule. To avoid further movement of the molecule, the tip was retracted

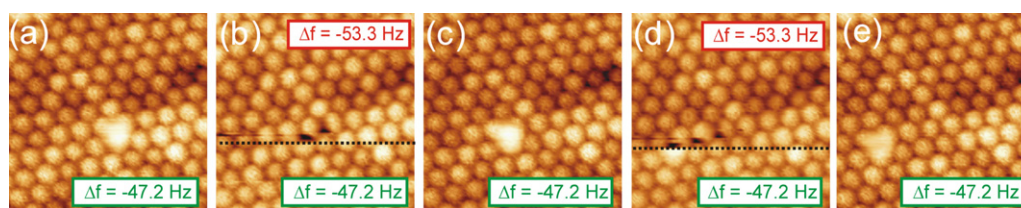


**Figure 3.** Tip-induced displacement of a water molecule along the slow scan direction measured at 80 K. (a) Water molecule imaged at a set point that leaves the molecule unperturbed at the surface. (b) The set point was changed beyond the tip–surface interaction threshold required to induce the movement of the water molecule, and the surface was scanned (above dotted line) until a jump to a first neighbouring binding site was detected; at which point the set point was switched back to the imaging conditions in (a) (below dotted line). (c) The molecule was imaged unperturbed at its new binding site. The process was repeated in (d), allowing the water molecule to diffuse over two consecutive binding sites, as confirmed in the image shown in (e). Displacement events appear as truncated dark pits at each of the binding sites visited by the water molecule. Image size  $(3.7 \times 3.7) \text{ nm}^2$ . Acquisition parameters  $f_0 = 150\,940 \text{ Hz}$ ,  $A = 7.1 \text{ nm}$ ,  $k = 24.6 \text{ N m}^{-1}$ . These images were taken with the same cantilever as used for taking the series of images shown in figure 2 but with a modified tip apex.

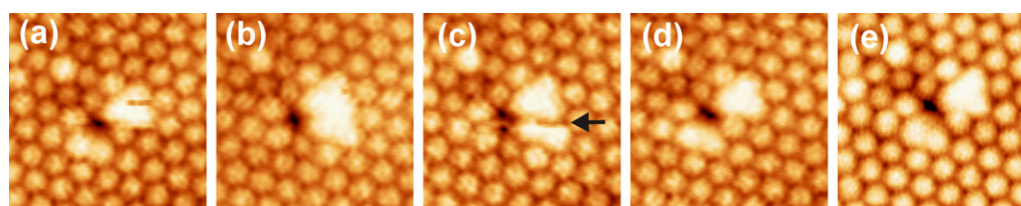


**Figure 4.** Series of successively recorded images (a)–(e) showing the tip-induced diffusion of a water molecule around a surface oxygen vacancy recorded at 80 K. The black arrow in (c) marks the line for the tip-induced movement. Image size  $(3 \times 3) \text{ nm}^2$ . Acquisition parameters  $f_0 = 150\,936 \text{ Hz}$ ,  $A = 8.7 \text{ nm}$ ,  $k = 24.6 \text{ N m}^{-1}$ ,  $\Delta f = -41.6 \text{ Hz}$ .

to the imaging conditions in figure 3(a) at the scan line indicated by the dotted line. Imaging the water molecule in the following frame (figure 3(c)) confirms that the molecule has migrated to a nearest neighbour equivalent binding site in the slow scan direction. The displacement is reproducible and demonstrated for the same water molecule again in the image shown in figure 3(d). In this image the water molecule is scanned again at a tip–surface distance below the threshold to induce the molecule displacement. Three black pits appeared, and switching back to imaging conditions directly resulted in visualizing the water molecule at a new position. The new location is confirmed by the image shown in figure 3(e), recorded at an identical set point as in figure 3(a). In total, within the series in figure 3, the tip-induced three jumps of the water molecule to nearest neighbour positions. By switching the set point between imaging and displacement conditions, one can control the movement of the molecule. The type of displacement presented above is similar to what has been observed for water on the  $\text{CaF}_2(111)$  surface [23], as well as for some semiconductor systems [19]. However, for this mode of scanning upwards or downwards, it is difficult to manipulate the molecule in a well-controlled fashion or position it on any desired location at the surface.

In the series of images shown in figure 4, tip-induced diffusion of a water molecule around a surface oxygen vacancy is displayed. Figure 4(a) shows the surface oxygen vacancy with two water molecules adsorbed near it. One water molecule is located at the right side of the vacancy while the second water molecule is located at the lower left side of the vacancy. The latter water molecule is adsorbed in a hollow site immediately close to the surface oxygen vacancy,

so that one of the vertices of the triangular structure ascribed to a water molecule appears truncated because of the absence of a surface oxygen atom; only two of the three equivalent neighbouring configurations available for the molecule around the hollow site [34] are visited by the water molecule. In a subsequent image, the water molecule originally positioned at the lower left side of the vacancy was perturbed by the tip during the scan, and it relocates on the right side of the vacancy, leading to the formation of a water dimer (see figure 4(b)). The image in figure 4(c) immediately follows the one displayed in figure 4(b) (scanning from bottom to top), and it reveals a second displacement of the water molecule induced by the tip at the position indicated by the arrow. Further imaging shows the molecule at its initial adsorption site that appears to be stable during subsequent scanning figure 4(e).

Another type of tip-induced dynamic process is the splitting of a water dimer. Clustering of water molecules is frequently observed upon significant water dosage [33]. An NC-AFM image of a water dimer structure measured at 80 K is shown in figures 5(a) and (b). The shape of the dimer structure suggests that it consists of two individual water molecules strongly bound to the surface and spaced by only one lattice constant, so that their triangular features share one of the underlying surface oxygen atoms. This is highlighted by the dashed and solid line representing the shape of each of the water molecules within the structure of the dimer. Scanning the same surface area, but at a higher tip–surface interaction, resulted in a tip instability (not shown). After recovery of the tip to yield atomic resolution, subsequent images acquired over the same surface area (figures 5(c) and (d)) showed

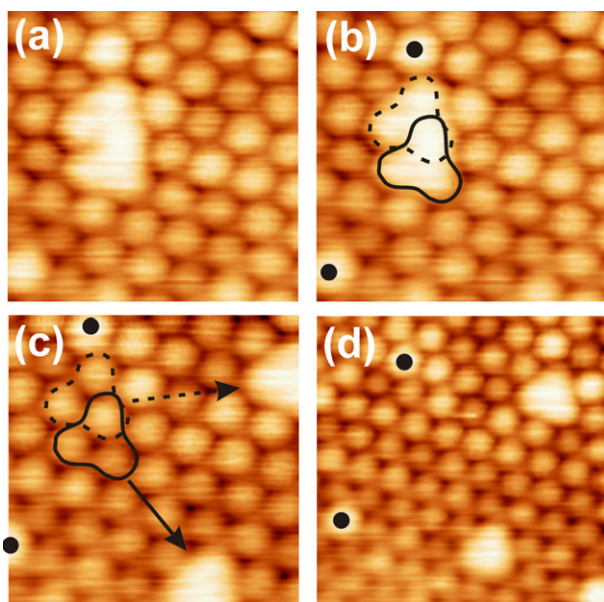


**Figure 5.** Image series showing the tip-induced splitting of a water dimer recorded at 80 K. The dimer imaged in (a), (b) was split by scanning at a higher tip–surface interaction than for the imaging conditions in (a) (not shown), resulting in the two isolated water molecules shown in (c), (d). Image sizes (a)–(c)  $(2.5 \times 2.5) \text{ nm}^2$  and (d)  $(3.4 \times 3.4) \text{ nm}^2$ . Acquisition parameters  $f_0 = 150\,567 \text{ Hz}$ ,  $k = 24.4 \text{ N m}^{-1}$ ,  $A = 11.0 \text{ nm}$ ,  $\Delta f = -87.7 \text{ Hz}$ .

the splitting of the dimer structure into two isolated water molecules. This finding indicates that the dimer structure displayed in figure 5(a) is indeed composed of two water molecules adsorbed on adjacent hollow sites, as indicated in figure 5(b).

## 5. Controlled lateral manipulation of individual water molecules

While the experiments discussed so far allow the displacement of individual water molecules on the  $\text{CeO}_2(111)$  surface, they do not enable a precise positioning of the molecule at any desired surface location, in the sense of a true molecular manipulation. A protocol which proves to be better suited for the controlled manipulation of individual water molecules is schematically shown in figure 6; this protocol is based on a previously reported procedure for the room temperature manipulation of individual atoms on semiconductor surfaces [20, 21]. First, an image of the molecule to be manipulated is taken as a reference, where the molecule is centred in the image. Afterwards, the same region is scanned again; however, as soon as the centre of the molecule is reached, the tip movement in the slow scan direction is stopped. Thus, upon further scanning, the same line is scanned in forward and backward fast scan directions atop the molecule as schematically shown in figure 6(a). In a second step, the tip is lifted high enough for the tip–surface short-range interaction to become negligible during the fast scan backward direction, as illustrated in figure 6(b). In a subsequent step, the tip–surface short-range interaction is

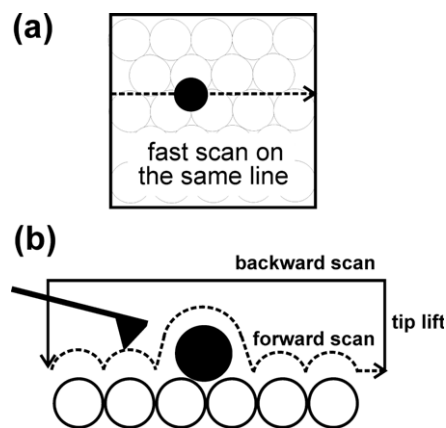


**Figure 6.** Protocol for molecular manipulation along the fast scan direction. (a) The scan in the slow direction is stopped on top of the structure to be manipulated and the same line is repetitively scanned. (b) A single scan line is then scanned in the forward direction, while in the backward direction the tip is lifted sufficiently high so that there is a negligible short-range interaction between tip and surface. During repetitive scans over the same line, the set point is stepwise increased until an instability in the topographic signal is observed. The set point is then immediately reduced to avoid any further manipulation.

stepwise increased in the fast scanning forward direction by successively decreasing the tip–surface separation until an instability in the topographic signal is registered. In this moment, the tip is immediately retracted from the surface to normal imaging conditions to avoid further manipulation events. Finally, the same surface area is imaged again at a tip–surface interaction below the threshold for the manipulation of the molecule to corroborate that the manipulation has been performed and the new location of the molecule is the desired one. By choosing a certain scanning angle with respect to the substrate surface directions, the intended direction of manipulation can be adjusted and the final position of the molecule can be determined among the available surrounding nearest neighbour binding sites.

The controlled manipulation of a single water molecule adsorbed on the  $\text{CeO}_2(111)$  surface performed at a tip–substrate temperature of 80 K according to this protocol is demonstrated in figure 7. The survey image in figure 7(a) shows two water molecules and a slightly protruding atom in the vicinity of the molecules that is highlighted by a black dot and used as a position marker. A higher resolution reference image shown in figure 7(b) is taken over the water molecule on the left. This image was then scanned again from bottom to top, and at the position marked with the black arrow in figure 7(c)—which corresponds to the centre position of the water molecule as shown by the arrow in figure 7(b)—the movement of the tip in the slow scan direction was stopped, resulting in a repetitive imaging of the same scan line, and the fast scan was set so that the tip is lifted several ångströms during the backward scan direction. The set point was then increased until an instability in the topographic signal was detected (upper arrow in figure 7(c)). Afterwards, the set point was reduced, and the imaging in the slow scan direction

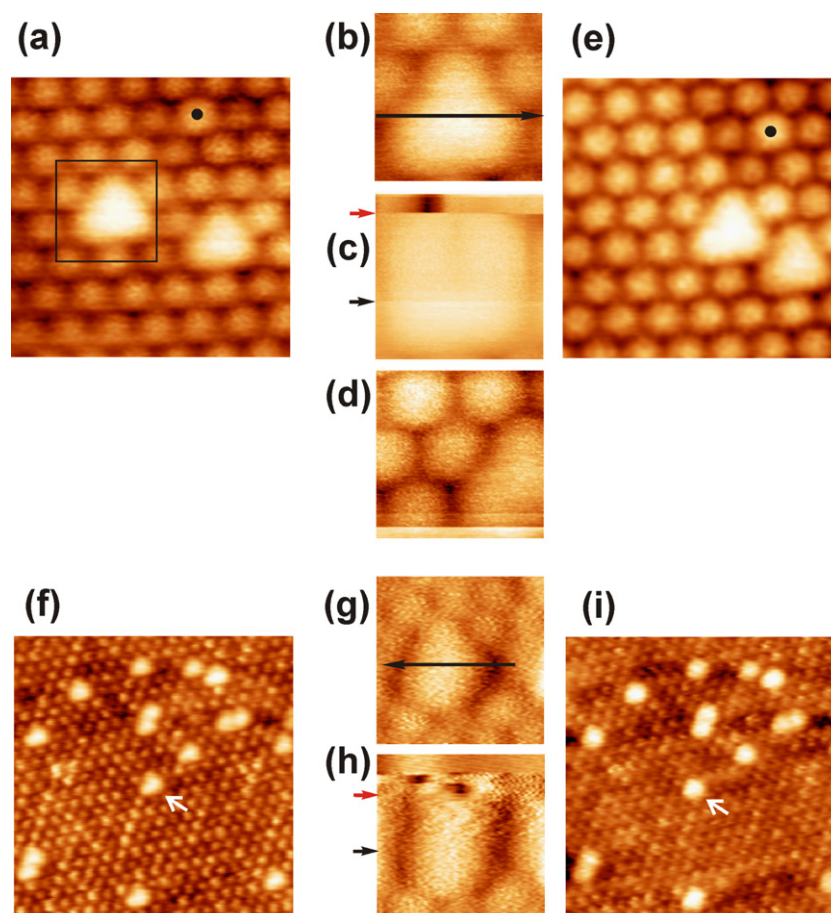


**Figure 7.** Controlled lateral manipulation of individual water molecules at a tip–surface temperature of 80 K (a)–(e) and at room temperature (f)–(i). (a) Two molecules before the manipulation. (b) Zoom over the water molecule on the left as indicated by the rectangle in (a). (c) Same image as in (b), until reaching the scan line indicated by the arrow, at which the slow scan was stopped, and the same line was scanned repetitively increasing the tip–surface interaction in the forward direction while lifting the tip up in the backward direction, as shown in figure 6. The arrow in the upper part of the image marks an instability in the topographic signal, characteristic of a successful manipulation event. (d) Same area as in (b). (e) Larger scale image showing the same area as in (a) after the manipulation. The dots in (a) and (e) mark the same atom for comparison of both images. (f) Image of a large surface area showing several water molecules adsorbed at room temperature. (g) Zoom over the water molecule indicated by the arrow in (f). (h) Same as in (g), yet at the position marked by the black arrow the slow scan was stopped and the tip–surface interaction was successively increased until an instability in the topography (marked by the red arrow) was observed. (i) Same area as in (f) after the manipulation. Image sizes (a) and (e)  $(2.7 \times 2.7) \text{ nm}^2$ , (b)–(d)  $(1.0 \times 1.0) \text{ nm}^2$ , (f) and (i)  $(8.0 \times 8.0) \text{ nm}^2$ , (g) and (h)  $(1.5 \times 1.5) \text{ nm}^2$ . Acquisition parameters (a)–(e)  $f_0 = 150\,567 \text{ Hz}$ ,  $k = 24.4 \text{ N m}^{-1}$ ,  $A = 11.0 \text{ nm}$ ,  $\Delta f = -25.3 \text{ Hz}$ ; (f)–(i)  $f_0 = 263\,852 \text{ Hz}$ ,  $k = 40 \text{ N m}^{-1}$ ,  $A = 16.9 \text{ nm}$ ,  $\Delta f = -35 \text{ Hz}$ . Manipulation of the water molecule was accomplished when increasing the set point from imaging conditions to  $-42 \text{ Hz}$  in (c) and to  $-45 \text{ Hz}$  in (h), respectively.

was continued. A subsequent reference image, taken over the same surface area as for figure 7(b), already indicates that the water molecule has been manipulated in the intended direction (figure 7(d)). Finally, the survey image presented in figure 7(e) yields evidence for the manipulation of the left water molecule by one lattice constant towards the other water molecule.

A similarly controlled lateral manipulation of individual water molecules can also be performed at room temperature, as shown in figures 7(f)–(i). Figure 7(f) is again the reference image of a group of water molecules adsorbed on the  $\text{CeO}_2(111)$  surface at room temperature. Figure 7(g) shows a zoom over the selected water molecule marked by the arrow in figure 7(f). The controlled manipulation over the fast scan direction (right to left in this case) is shown in figure 7(h). Here, the tip is lifted when travelling from left

to right. As in the previous example, the position where the tip slow scan movement was stopped is marked by a black arrow and the line scan at which an instability associated with the manipulation of the molecule after successively increasing the tip–surface interaction force is marked by a red arrow. In the large scale image shown in figure 7(i), corresponding to the same surface area displayed in figure 7(f), the new position of the manipulated molecule (white arrow) with respect to the rest of the water molecules can be seen. Due to the thermal energy involved in room temperature manipulation experiments, in some cases and for some tip apex terminations, the manipulation processes is somewhat less controlled than in the case of low temperature experiments. More frequently than in low temperature experiments, the molecule is found

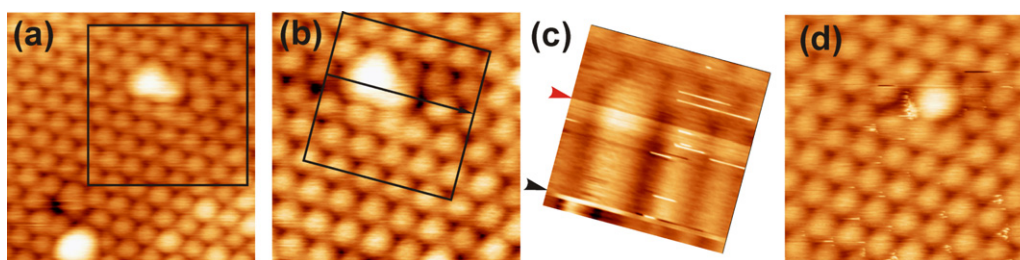


**Figure 8.** Lateral manipulation of a water molecule across a surface oxygen vacancy performed at 80 K. (a) Overview image showing two surface oxygen vacancies [32] and two water molecules (one on the top and another at the bottom of the image) next to each of the vacancies. (b) Zoom in over the upper water molecule as indicated by the rectangle depicted in (a). (c) Image acquired over the surface area marked by the rectangle in (b), showing the process of manipulating the water molecule towards the surface oxygen vacancy. At the position marked by the upper arrow, the slow scan was stopped and the tip–surface interaction was progressively increased until an instability in the topography was recorded (lower arrow). (d) Image showing the new position of the manipulated water molecule with respect to the surface oxygen vacancy. Image sizes (a)  $(4.0 \times 4.0) \text{ nm}^2$ , (b) and (d)  $(3.0 \times 3.0) \text{ nm}^2$ , (c)  $(1.8 \times 1.8) \text{ nm}^2$ . Acquisition parameters  $f_0 = 170\,729 \text{ Hz}$ ,  $k = 34.8 \text{ N m}^{-1}$ ,  $A = 11.0 \text{ nm}$ ,  $\Delta f = -60 \text{ Hz}$ . Manipulation of the water molecule was accomplished when increasing the set point from imaging conditions to  $-66 \text{ Hz}$ .

to move in an unintended direction, i.e. not in front of the tip but around it. Furthermore, attempts at controlled lateral manipulations of water molecules performed at room temperature more frequently result in picking up the desired water molecule by the tip during the manipulation process. Nonetheless, our manipulation experiments clearly demonstrate that, according to the manipulation protocol reported here, a precise site-by-site manipulation of individual water molecules adsorbed on the  $\text{CeO}_2(111)$  surface is feasible at both cryogenic and room temperatures.

It has been predicted that a water molecule adsorbed at a surface oxygen vacancy of the  $\text{CeO}_2(111)$  surface would spontaneously dissociate [34]. We have tried to induce and characterize the dissociation of an individual water molecule by manipulating it towards a surface oxygen vacancy, as exemplified in figure 8, using the manipulation protocol described above. Figure 8(a) shows a surface area with two surface oxygen vacancies [32] and two water molecules, each of them adsorbed close to the corresponding vacancy. Figure 8(b) is a zoom over the upper molecule/vacancy pair marked by a rectangle in (a), where the intended manipulation direction is marked by an arrow. Figure 8(c) corresponds to the area marked by the rectangle in figure 8(b) (the scan frame has been rotated to align the fast scan direction parallel to the intended manipulation direction), and it shows the application of the manipulation protocol described above. The image in figure 8(d) demonstrates the completed manipulation event. A comparison of the water and vacancy positions before (figure 8(b)) and after (figure 8(d)) the manipulation process yields the atomic positions near the surface vacancy. This experiment demonstrates that the water molecule can also be manipulated in the vicinity of the vacancy, and that the water molecule may rest at a position that is, in fact, partially overlapping with the vacancy, as is also displayed in figure 4. In spite of many manipulation events performed to try to induce the adsorption of the water molecule inside the surface oxygen vacancy, we have always observed that the water molecule prefers to bind at a position surrounding the vacancy instead of getting inside the vacancy or being dissociated during the manipulation.

## 6. Conclusions

In conclusion, we have demonstrated the controlled manipulation of individual water molecules adsorbed on the (111) surface of cerium dioxide—a truly insulating material—at temperatures as low as 80 K, as well as at room temperature. To achieve a controlled manipulation, the tip is brought into close proximity with the molecule and a strong force in the desired manipulation direction is exerted on the molecule by the movement of the tip. Our results suggest that the tip-induced displacement of the water molecule is a hopping motion, since only the initial and final positions of the manipulated molecule are imaged at both 80 K and room temperature. It is very likely that the presence of the tip during imaging at significant tip–surface interaction forces would lower the energy barrier for the diffusion of the water molecule on the  $\text{CeO}_2(111)$  surface, which eventually leads to thermally assisted manipulation [17, 20, 21] of the water molecule to the nearest neighbour adsorption positions. This hopping displacement explains why water molecules are sometimes found to move in the opposite direction of the tip scan in manipulation experiments following the manipulation protocol described above. It is worth mentioning that the interaction of the tip with the substrate and the water molecules throughout all of the experiments is attractive. This provides a straightforward explanation for water molecules sometimes being picked up by the tip during manipulation attempts.

Another interesting aspect of our studies is the observation that water molecules may form apparent dimers or clusters at the surface but we never observe the formation of a stable molecular structure as one would intuitively expect in view of the ability of water molecules to form a hydrogen-bonded network. Rather we find that it is quite easy to separate two incidentally neighbouring water molecules by the action of the AFM tip.

## Acknowledgments

This work has been supported by the Deutsche Forschungsgemeinschaft (grant no. 446 JAP 113/337/322/0-1), by

a Grant-in-Aid for Scientific Research on Priority Areas (grant no. 19053006) from the Ministry of Education, Culture, Sports, Science and Technology (MEXT) and by a Grant-in-Aid for Scientific Research (S) (grant no. 22221006) from the Japan Society for the Promotion of Science (JSPS).

## References

- [1] Feynman R P 1960 There's plenty of room at the bottom *Eng. Sci.* **23** 22–36
- [2] Strosio J and Eigler D M 1991 Atomic and molecular manipulation with the scanning tunneling microscope *Science* **254** 1319–26
- [3] Meyer G, Repp J, Zöphel S, Braun K-F, Hla S W, Fölsch S, Bartels L, Moresco F and Rieder K H 2000 Controlled manipulation of atoms and small molecules with a low temperature scanning tunneling microscope *Single Mol.* **1** 79–86
- [4] Ho W 2002 Single-molecule chemistry *J. Chem. Phys.* **117** 11033–61
- [5] Moresco F 2004 Manipulation of large molecules by low-temperature STM: model systems for molecular electronics *Phys. Rep.* **399** 175–225
- [6] Butcher M J, Jones F H, Moriarty P, Beton P H, Prassides K, Kordatos K and Tagmatarchis N 1999 Room temperature manipulation of the heterofullerene C<sub>59</sub>N on Si(100)-2 × 1 *Appl. Phys. Lett.* **75** 1074–6
- [7] Keeling D L, Humphry M J, Fawcett R H J, Beton P H, Hobbs C and Kantorovich L 2005 Bond breaking coupled with translation in rolling of covalently bound molecules *Phys. Rev. Lett.* **94** 146104
- [8] Martsinovich N, Kantorovich L, Fawcett R H J, Humphry M J and Beton P H 2008 Constrained molecular manipulation mediated by attractive and repulsive tip-adsorbate forces *Small* **4** 765–9
- [9] Chen C J 2008 *Introduction to Scanning Tunneling Microscopy* (New York: Oxford University Press)
- [10] Sugimoto Y, Nakajima Y, Sawada D, Morita K, Abe M and Morita S 2010 Simultaneous AFM and STM measurements on the Si(111)-(7 × 7) surface *Phys. Rev. B* **81** 245322
- [11] Ternes M, Gonzalez C, Lutz C P, Hapala P, Giessibl F J, Jelinek P and Heinrich A J 2011 Interplay of conductance, force, and structural change in metallic point contacts *Phys. Rev. Lett.* **106** 016802
- [12] Weymouth A J, Wutscher T, Welker J, Hofmann T and Giessibl F J 2011 Phantom force induced by tunneling current: a characterization on Si(111) *Phys. Rev. Lett.* **106** 226801
- [13] Grill L, Rieder K-H, Moresco F, Stojkovic S, Gourdon A and Joachim C 2006 Exploring the interatomic forces between tip and single molecules during STM manipulation *Nano Lett.* **6** 2685–9
- [14] Ternes M, Lutz C P, Hirjibehedin C F, Giessibl F J and Heinrich A J 2008 The force needed to move an atom on a surface *Science* **319** 1066–9
- [15] Custance O, Pérez R and Morita S 2009 Atomic force microscopy as a tool for atom manipulation *Nature Nanotechnol.* **4** 803–10
- [16] Oyabu N, Custance O, Yi I, Sugawara Y and Morita S 2003 Mechanical vertical manipulation of selected single atoms by soft nanoindentation using near contact atomic force microscopy *Phys. Rev. Lett.* **90** 176102
- [17] Sugimoto Y, Pou P, Custance O, Jelinek P, Abe M, Pérez R and Morita S 2008 Complex patterning by vertical interchange atom manipulation using atomic force microscopy *Science* **322** 413–7
- [18] Sweetman A, Jarvis S, Danza R, Bamidele J, Gangopadhyay S, Shaw G A, Kantorovich L and Moriarty P 2011 Toggling bistable atoms via mechanical switching of bond angle *Phys. Rev. Lett.* **106** 136101
- [19] Oyabu N, Sugimoto Y, Abe M, Custance O and Morita S 2005 Lateral manipulation of single atoms at semiconductor surfaces using atomic force microscopy *Nanotechnology* **16** S112–7
- [20] Sugimoto Y, Abe M, Hirayama S, Oyabu N, Custance O and Morita S 2005 Atom inlays performed at room temperature using atomic force microscopy *Nature Mater.* **4** 156–9
- [21] Sugimoto Y, Jelinek P, Pou P, Abe M, Morita S, Pérez R and Custance O 2007 Mechanism for room-temperature single-atom lateral manipulations on semiconductors using dynamic force microscopy *Phys. Rev. Lett.* **98** 106104
- [22] Nishi R, Miyagawa D, Seino Y, Yi I and Morita S 2006 Non-contact atomic force microscopy study of atomic manipulation on an insulator surface by nanoindentation *Nanotechnology* **17** S142–7
- [23] Hirth S, Ostendorf F and Reichling M 2006 Lateral manipulation of atomic size defects on the CaF<sub>2</sub>(111) surface *Nanotechnology* **17** S148–54
- [24] Gorte R J 2010 Ceria in catalysis: from automotive applications to the water gas shift reaction *AIChE J.* **56** 1126–35
- [25] Beckers J and Rothenberg G 2010 Sustainable selective oxidations using ceria-based materials *Green Chem.* **12** 939–48
- [26] Lin K S and Chowdhury S 2010 Synthesis, characterization, and application of 1D cerium oxide nanomaterials: a review *Int. J. Mol. Sci.* **11** 3226–51
- [27] Celardo I, Pedersen J Z, Traversa E and Ghibelli L 2011 Pharmacological potential of cerium oxide nanoparticles *Nanoscale* **3** 1411–20
- [28] Lauritsen J V and Reichling M 2010 Atomic resolution non-contact atomic force microscopy of clean metal oxide surfaces *J. Phys.: Condens. Matter* **22** 263001
- [29] Gritschneider S, Namai Y, Iwasawa Y and Reichling M 2005 Structural features of CeO<sub>2</sub>(111) revealed by dynamic SFM *Nanotechnology* **16** S41–8
- [30] Torbrügge S, Cranney M and Reichling M 2008 Morphology of step structures on CeO<sub>2</sub>(111) *Appl. Phys. Lett.* **93** 073112
- [31] Gritschneider S and Reichling M 2008 Atomic resolution imaging on CeO<sub>2</sub>(111) with hydroxylated probes *J. Phys. Chem. C* **112** 2045–9
- [32] Torbrügge S, Reichling M, Ishiyama A, Morita S and Custance O 2007 Evidence of subsurface oxygen vacancy ordering on reduced CeO<sub>2</sub>(111) *Phys. Rev. Lett.* **99** 056101
- [33] Gritschneider S, Iwasawa Y and Reichling M 2007 Strong adhesion of water to CeO<sub>2</sub>(111) *Nanotechnology* **18** 044025
- [34] Watkins M B, Foster A S and Shluger A L 2007 Hydrogen cycle on CeO<sub>2</sub>(111) surfaces: density functional theory calculations *J. Phys. Chem. C* **111** 15337–41
- [35] Fronzi M, Piccinin S, Delley B, Traversa E and Stampfl C 2009 Water adsorption on the stoichiometric and reduced CeO<sub>2</sub>(111) surface: a first-principles investigation *Phys. Chem. Chem. Phys.* **11** 9188–99
- [36] Foster A S, Trevethan T and Shluger A L 2009 Structure and diffusion of intrinsic defects, adsorbed hydrogen, and water molecules at the surface of alkali-earth fluorides calculated using density functional theory *Phys. Rev. B* **80** 115421
- [37] Torbrügge S, Lübke J, Tröger L, Cranney M, Eguchi T, Hasegawa Y and Reichling M 2008 Improvement of a dynamic scanning force microscope for highest resolution imaging in ultrahigh vacuum *Rev. Sci. Instrum.* **79** 083701

- [38] Lübke J, Tröger L, Torbrügge S, Bechstein R, Richter C, Kühnle A and Reichling M 2010 Achieving high effective Q-factors in ultra-high vacuum dynamic force microscopy *Meas. Sci. Technol.* **21** 125501
- [39] Gritschneider S and Reichling M 2007 Structural elements of CeO<sub>2</sub>(111) surfaces *Nanotechnology* **18** 044024
- [40] Sadewasser S, Jelinek P, Fang C K, Custance O, Yamada Y, Sugimoto Y, Abe M and Morita S 2009 New insights on atomic-resolution frequency-modulation kelvin-probe force-microscopy imaging of semiconductors *Phys. Rev. Lett.* **103** 266103
- [41] Mitsui T, Rose M K, Fomin E, Ogletree D F and Salmeron M 2002 Water diffusion and clustering on Pd(111) *Science* **297** 1850–2
- [42] Custance O, Brochard S, Brihuega I, Artacho E, Soler J M, Baro A M and Gomez-Rodriguez J M 2003 Single adatom adsorption and diffusion on Si(111)-(7 × 7) surfaces: scanning tunneling microscopy and first-principles calculations *Phys. Rev. B* **67** 235410
- [43] Rahe P, Bechstein R, Schütte J, Ostendorf F and Kühnle A 2008 Repulsive interaction and contrast inversion in noncontact atomic force microscopy imaging of adsorbates *Phys. Rev. B* **77** 195410